Damage mechanisms for ultrasound-induced cavitation in tissue

M. Warnez*, E. Vlaisavljevich†, Z. Xu† and E. Johnsen*

*Department of Mechanical Engineering, University of Michigan, Ann Arbor, MI
†Department of Biomedical Engineering, University of Michigan, Ann Arbor, MI

Abstract.
In a variety of biomedical applications, cavitation occurs in soft tissue. Although significant amounts of research have been performed on cavitation in water, bubble dynamics, and related bioeffects remain poorly understood. We use numerical simulations of spherical bubble dynamics in soft tissue to assess the extent to which viscoelasticity affects "known" and introduces "new" damage mechanisms. We find that deviatoric stresses – although not an important damage mechanism in water – are significantly enhanced and could be an important bioeffect mechanism in tissue. Both the viscoelastic properties and the nonlinear, large-collapse radius contribute to stress amplification in the surroundings. In addition, temperatures in the surrounding medium increase more in the Zener tissue than in water, due to viscous heating.

Keywords: Cavitation, bubble dynamics, viscoelastic media, soft tissue, cavitation bioeffects
PACS: 47.55.dd, 47.55.dp, 87.50.yg, 87.50.yt

INTRODUCTION

Cavitation plays an important role in a variety of applications in medicine. In diagnostic ultrasound, contrast may be improved by injecting microbubbles [7]. In therapeutic ultrasound, e.g., shock-wave lithotripsy [12], high-intensity focused ultrasound [18] or histotripsy [17], bubbles form and respond to the incoming pulses. In these applications, cavitation bubbles may be produced directly in soft tissue, a viscoelastic medium. While bubble dynamics research in water has received significant attention in both hydrodynamic [3] and acoustic [11] cavitation, the behavior of bubbles in viscoelastic tissue-like media is much less well understood, as the bubble dynamics are strongly affected by varying non-Newtonian properties of their surroundings. Theoretical and numerical investigations have primarily focused on investigating the basic mechanics of cavitation bubbles, in Maxwell-like [1, 2], Kelvin-Voigt-like [21, 9] and general viscoelastic media [20]. These studies have shown that the bubble dynamics strongly depend on the constitutive model and properties. One of the important outcomes of cavitation is damage to the surroundings, which has motivated a significant amount of research in hydrodynamic applications [3]. While the precise damage mechanism remains unknown, inertial cavitation-bubble collapse can produce high transient pressures and temperatures, shock waves and, in the case of non-spherical collapse, re-entrant jets. All of these mechanisms have the potential to destroy neighboring solid objects. In the biomedical world, it is known that cavitation can lead to biological effects [4, 14], a number of which are attributed to cavitation. However, few studies have sought to connect the mechanics of bubbles in tissue to potential damage or bioeffects. The response of microbubbles to diagnostic ultrasound waveforms indicate a strong dependence of bioeffects on the pulse properties (specifically frequency) and viscoelastic properties [15]. Given that tissue behaves in a viscoelastic fashion, it is unclear whether traditional mechanisms are expected to cause damage. The overall objective of this work is to provide a better understanding of cavitation-induced damage in viscoelastic media. Specifically, we use numerical simulations of spherical bubble dynamics in soft tissue to assess the extent to which viscoelasticity affects "known" and introduces "new" damage mechanisms.

BUBBLE DYNAMICS IS SOFT TISSUE

The Keller-Miksis equation

$$\left(1-\frac{\dot{R}}{c}\right)R\ddot{R}+\frac{3}{2}\left(1-\frac{\dot{R}}{3c}\right)\dot{R}^2=\frac{1}{\rho}\left(1+\frac{\dot{R}}{c}+\frac{R}{c}\frac{d}{dt}\right)\left(p_B-\frac{2S}{R}+J-p_\infty-p_a(t)\right) \quad (1)$$

Proceedings from the 14th International Symposium on Therapeutic Ultrasound
AIP Conf. Proc. 1821, 080004-1–080004-5; doi: 10.1063/1.4977634
Published by AIP Publishing. 978-0-7354-1489-1/$30.00

describes the evolution of a spherical bubble of radius R in an infinite, incompressible medium with density ρ, ambient pressure p_∞, and sound speed c. The bubble, with spatially-uniform internal pressure p_B and constant surface tension S, is subjected to an acoustic pressure forcing p_a, which is taken as a known function of time t. The bubble is also influenced by the viscoelastic deviatoric stresses in the medium through the quantity $J = 2\int_R^\infty \frac{\tau_{rr}-\tau_{\theta\theta}}{r}\,dr$ which integrates over the difference in radial (τ_{rr}) and polar ($\tau_{\theta\theta}$) normal stresses. To compute the stresses in the tissue, a constitutive model must be assumed. As a starting place for modeling the tissue rheology, we use the Zener solid (or standard linear solid) model, which is the simplest constitutive model to combine viscosity μ, elasticity G, and relaxation time λ_1. The Zener model linearly relates the deviatoric stress tensor $\boldsymbol{\tau}$ and its time derivative to that of the infinitesimal strain tensor and its time derivative. The normal stresses in the radial direction are given by

$$\tau_{rr} + \lambda_1 \dot{\tau}_{rr} = -\frac{4}{r^3}\left[\frac{G}{3}\left(R^3 - R_0^3\right) + \mu R^2 \dot{R}\right] \tag{2}$$

while in the polar direction $\tau_{\theta\theta} = -\frac{1}{2}\tau_{rr}$. By spherical symmetry, $\tau_{\theta\theta} = \tau_{\phi\phi}$. In the spherical coordinate frame, all of the off-diagonal elements of $\boldsymbol{\tau}$ are zero.

As shown in our previous work [20], the Keller-Miksis equation for a bubble in a Zener solid can be solved in terms of the following three first-order ODEs:

$$\dot{R} = U \tag{3}$$

$$\dot{J} = -\left(\frac{1}{\lambda_1} + \frac{3U}{R}\right) J - \frac{4}{\lambda_1}\left[\frac{G}{3}\left(1 - \frac{R_0^3}{R^3}\right) + \mu \frac{U}{R}\right] \tag{4}$$

$$\dot{U} = \left[-\frac{3}{2}\left(1 - \frac{U}{3c}\right)U^2 + \frac{1}{\rho}\left(1 + \frac{U}{c}\right)\left(p_B - \frac{2S}{R} + J - p_\infty - p_a\right) + \frac{R}{\rho c}\left(\dot{p}_B + \frac{2SU}{R^2} + \dot{J} - \dot{p}_a\right)\right] \Big/ \left(R - \frac{RU}{c}\right). \tag{5}$$

In this work, the internal bubble pressure is calculated using Prosperetti's detailed heat transfer model [16, 10], which requires solving partial differential equations for the temperature fields inside and outside the bubble. The method described in our previous work [20] is used for this purpose.

Zener viscoelasticity introduces three additional parameters into the bubble model. Rather than study the parametric dependence of the bubble response on the viscoelastic properties, we herein make a detailed investigation into the physics of a single case study. The base case is chosen to be representative of the physical situation of cavitation-induced ultrasound. The bubble is initiated in equilibrium, with radius $R_0 = 1.0\,\mu$m, and filled with air having constant ratio of specific heats of 1.4. The bubble is then subjected to a sinusoidal acoustic forcing pressure with amplitude 400 kPa and frequency 3.0 MHz. This forcing pressure corresponds to a low-amplitude ultrasound wave. Unfortunately, the viscoelastic properties of tissue are largely unknown, and are expected to vary greatly between tissues types. Here we choose parameters that fall in the range of typical tissue viscosity and elasticity: $\mu = 30$ cP and $G = 10$ kPa. Little has been measured concerning the relaxation time of tissue, so we choose a value $\lambda_1 = 0.1\,\mu$s that abides by the inequality $\lambda_1 < \mu/G$, which is mandated by the Zener model [9]. The surface tension, also largely unknown, was taken to be that of blood, $S = 0.056\,\mathrm{N/m}$.

Fig. 1 shows the bubble response in Zener tissue, compared to the bubble response in water ($\mu = 1.0$ cP), subjected to the same acoustic pressure. While the bubbles oscillate at the same frequency and have a comparable maximum radius, the bubble in water collapses down to a much smaller radius before rebounding. Since the important physics typically occurs during bubble collapse, these bubble responses are expected to induce very different effects in the surroundings. The water bubble experiences larger radial strains during collapse due to the small collapse radius. While the water bubble causes compressive polar strains at collapse, the tissue surrounding the Zener bubble is still in tension in the polar direction during collapse. Since the time scales in which these strains evolve are very short, the tissue surrounding the bubble undergoes very high strain rates. Strain rates are extremely high everywhere in the near field, in both directions. Radial train rates of up to 10^9 1/s are predicted on the wall of the water bubble, while strain rates in both directions for the Zener bubble reach 10^9 1/s.

Fig. 2 shows the temperature in the surrounding bubble between the two cases. In neither case do the high temperatures inside the bubble greatly affect the temperature in the surroundings. In fact, the temperatures are slightly higher in the Zener tissue case due to viscous heating, even though the bubble collapses are less forceful. Due to viscous heating, the rate of heat generation per unit volume in the surrounding medium is given by $\dot{q} = -3\frac{R^2\dot{R}}{r^3}\tau_{rr}(r,t)$. In a Newtonian fluid, this reduces to $\dot{q} = 12\mu\left(R^2\dot{R}/r^3\right)^2$. We suspect that the transient high temperatures are not likely

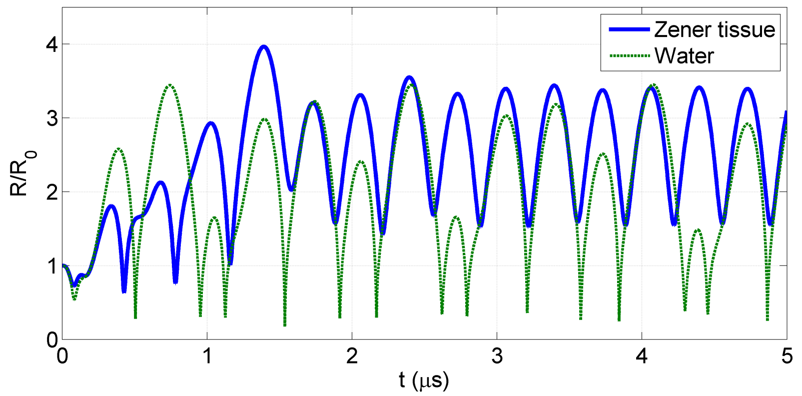

FIGURE 1. Bubble reponse to harmonic forcing in different surrounding media. Subjected to the same forcing, the bubble in water collapses to much smaller radii than the bubble in Zener tissue, even though the bubbles grow to comparable sizes.

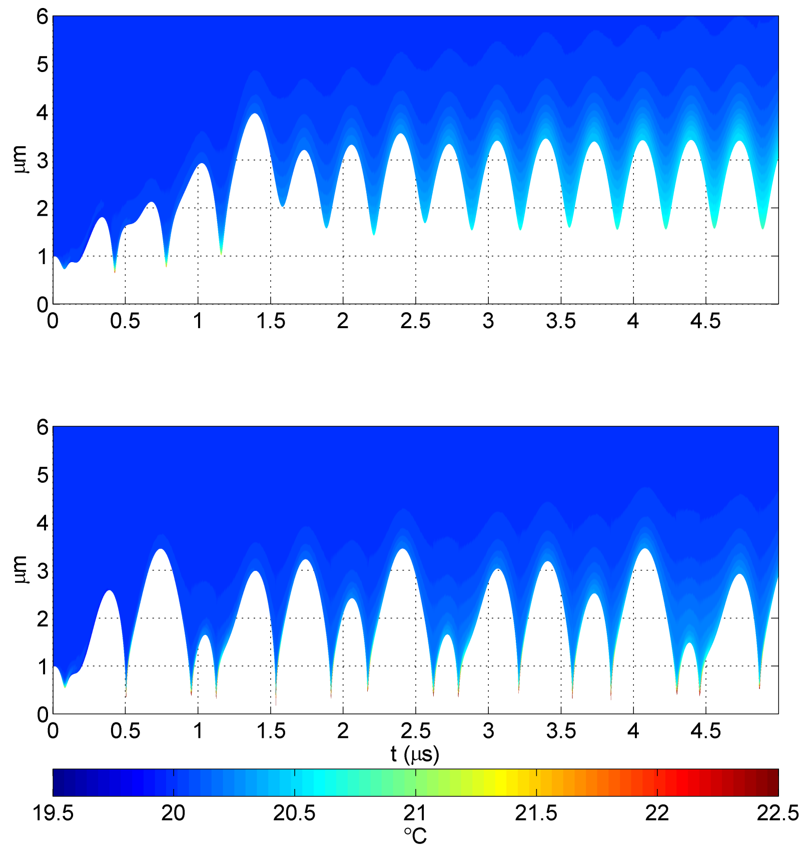

FIGURE 2. Temperature in the surroundings. The white area denotes the bubble response vs. time. Viscous heating is more significant in the Zener tissue, but very high temperatures are momentarily generated at the collapse instant in water.

to cause immediate ablation of cells. However, long-term oscillation of a cluster of such bubbles may cause enough viscous heating to mediate mild hyperthermia.

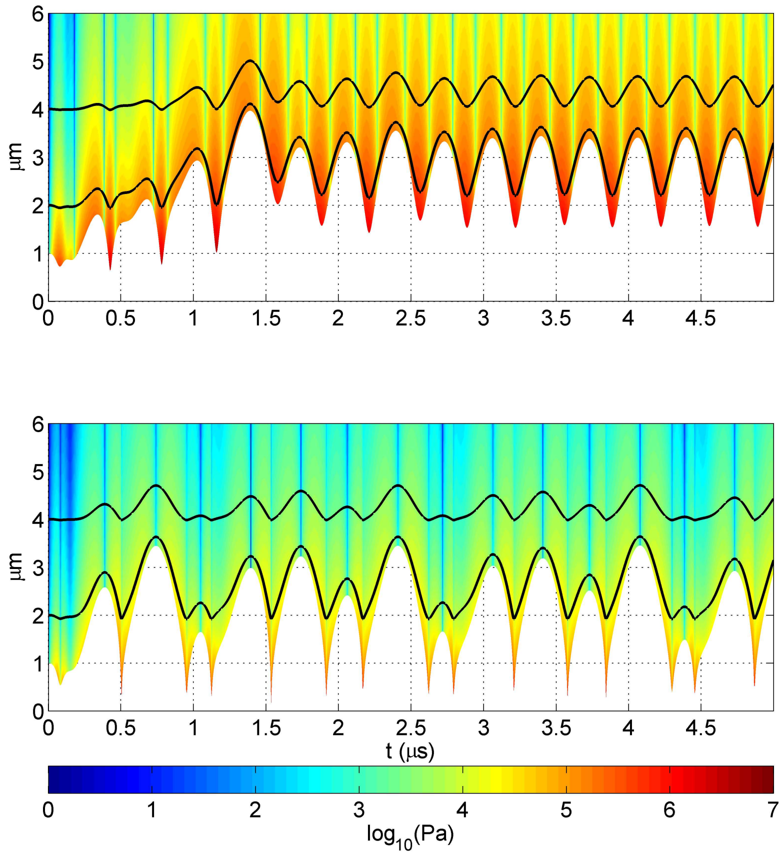

FIGURE 3. Contours of radial stresses at a given instant in time. The white area denotes the bubble response vs. time. The line denotes the path of a "particle" initially located at 1 and 3 μm away from the bubble. Significantly larger stresses are experienced by a particle in the viscoelastic medium.

Fig. 3 shows the radial stress fields. It is immediately clear that larger stresses are generated in the Zener tissue, even though larger pressures, strains, and strain rates are generated in the water case. This is due to the large values of the viscoelastic properties in the Zener tissue; tissue is more viscous and elastic than water, therefore, in tissue, the same strains generate larger stresses. The bubble wall motion is similar between the two cases, meaning the strains will be similiar, but much higher stresses appear in the Zener tissue.

It is also of note that the high stresses generated in the Zener tissue reach far into the surrounding material, while the high stresses in the water occur only at the collapse instant and very near to the bubble wall. The dark lines in the surrounding identifies the location of Lagrangian points, that is, points that are stationary with respect to the surrounding media. Such models the trajectory of a cell in the surroundings. The trajectory of a particle initially at a distance r_0 from the bubble center is given by $r(t) = \sqrt[3]{r_0^3 - R^3 - R_0^3}$. It is clear from following these trajectories that particles in the Zener tissue are much nearer to the bubble wall at the high-stress instant of collapse. This means that out-of-equilibrium oscillations could be responsible damage which is more far reaching.

Of course, the Zener tissue bubble behavior need not be the steady, out-of-equilibrium response in order for geometrical effects to amplify the stresses in the surroundings. At large forcing 2amplitudes, bubbles readily rebound at large radii, due to relaxation effects. This rebound can be very violent, and non-periodic. In water, bubble rebound is driven solely by pressure, whereas in relaxative materials, rebound can occur solely due to deviatoric stresses.

CONCLUSIONS

We use numerical simulations of spherical bubble dynamics in soft tissue to assess the extent to which viscoelasticity affects "known" and introduces "new" damage mechanisms. Our main conclusions are that deviatoric stresses – although not an important damage mechanism in water – are significantly enhanced and could be an important bioeffect mechanism in tissue. Both the viscoelastic properties and the nonlinear, large-collapse radius contribute to stress amplification in the surroundings. In addition, temperatures in the surrounding medium increase more in the Zener tissue than in water, due to viscous heating. If steady, nonviolent oscillations could possibly be used to control tissue heating in a variety of applications. However, temperature alone is not likely to be a damage mechanism in cavitation-induced cell death for the conditions under consideration.

ACKNOWLEDGMENTS

This work was supported in part by NSF grant number CBET 1253157 and NIH grant number 1R01HL110990-01A1.

REFERENCES

1. J. Allen and R. Roy, "Dynamics of gas bubbles in viscoelastic fluids. I. Linear viscoelasticity," J. Acoust. Soc. Am. **107**, 3167–3178 (2000a).
2. J. Allen and R. Roy, "Dynamics of gas bubbles in viscoelastic fluids. II. Nonlinear viscoelasticity," J. Acoust. Soc. Am. **108**, 1640–1650 (2000b).
3. C. E. Brennen, *Cavitation and Bubble Dynamics*. University Press, Oxford (1995).
4. D. Dalecki, "Mechanical bioeffects of ultrasound," Annu. Rev. Biomed. Eng. **6**, 229–248 (2004).
5. S. De, J. Rosen, A. Dagan, B. Hannaford, P. Swanson, and M. Sinanan, "Assessment of tissue damage due to mechanical stresses," The International Journal of Robotics Research **26**(11-12), 1159-1171 (2007).
6. H. G. Flynn, "Cavitation dynamics: II. Free pulsations and models for cavitation bubbles," J. Acoust. Soc. Am. **58**(6), 1160-1170 (1975).
7. B. B. Goldberg, J. B. Liu and F. Forsberg, "Ultrasound contrast agents: A review," Ultrasound Med. Biol. **20**, 319–333 (1994)
8. C.K. Holland, and R. E. Apfel, An improved theory for the prediction of microcavitation thresholds," IEEE T. Ultrason. Ferr. **36**(2), 204-208 (1989).
9. C. Hua and E. Johnsen, "Nonlinear oscillations following the Rayleigh collapse of a gas bubble in a linear viscoelastic (tissue-like) medium," Phys. Fluids **25**, 083101 (2013).
10. V. Kamath, A. Prosperetti, and F. N. Egolfopoulos, "A theoretical study of sonoluminescence," J. Acoust. Soc. Am. **94**(1), 248-260 (1993).
11. T. Leighton, *The Acoustic Bubble*. Academic Press, London (1994).
12. J. E. Lingeman, "Extracorporeal shock wave lithotripsy: development, instrument, and current status," Urol. Clin. North Am. **24**, 185–211 (1997).
13. D. Milentijevic, I. F. Rubel, A. S. Liew, D. L. Helfet, and P. A. Torzilli, "An in vivo rabbit model for cartilage trauma: a preliminary study of the influence of impact stress magnitude on chondrocyte death and matrix damage," Journal of Orthopaedic Trauma **19**(7), 466-473 (2005).
14. D. L. Miller, "Overview of experimental studies of biological effects of medical ultrasound caused by gas body activation and inertial cavitation", Prog. Biophys. Mol. Bio. **93** 314–330 (2007).
15. B. Patterson, D. L. Miller and E. Johnsen, "Theoretical microbubble dynamics in a viscoelastic medium at capillary breaching thresholds," J. Acoust. Soc. Am. **132**, 3770–3777 (2012).
16. A. Prosperetti, L. A. Crum, and K. W. Commander, "Nonlinear bubble dynamics," J. Acoust. Soc. Am. **83**, 502-514 (1988).
17. W. W. Roberts, T. L. Hall, K. Ives, J. S. Wolf Jr., J. B. Fowlkes and C. A. Cain, "Pulsed cavitational ultrasound: A noninvasive technology for controlled tissue ablation (histotripsy) in the rabbit kidney," J. Urol. **175**, 734–738 (2006).
18. G. ter Haar, D. Sinnett and I. Rivens, "High intensity focused ultrasound–A surfical technique for the treatment of discrete liver tumours," Phys. Med. Biol. **34**, 1743–1750 (1989).
19. P. A. Torzilli, J. Borrelli, D. L. Helfet, and R. Grigiene, "Effect of impact load on articular cartilage: cell metabolism and viability, and matrix water content," Journal of Biomechanical Engineering **121**(5), 433-441 (1999).
20. M. T. Warnez and E. Johnsen (2014), in preparation.
21. X. Yang and C. C. Church, "A model for the dynamics of gas bubbles in soft tissues," J. Acoust. Soc. Am. **118**, 3595–3606 (2005).